

Imaging assessment of tumor densities and sizes following pazopanib treatment for central nervous system solitary fibrous tumors with multiple extracranial metastases: A case series

TAKAYA TSUNO^{1,2}, NORITAKA MASAHIRA³, KUNIIHIKO NUMOTO⁴, HITOMI IWASA², NAO KAGIMOTO⁵, DAICHI YAMASAKI¹, YUICHIRO KONDO¹, TOSHIKI MATSUOKA¹ and HIROYUKI NISHIMURA¹

¹Department of Neurosurgery, Kochi Health Sciences Center, Kochi 781-8555, Japan; ²Department of Radiology, Kochi Health Sciences Center, Kochi 781-8555, Japan; ³Department of Neurosurgery, Hata Kenmin Hospital, Kochi 788-0785, Japan; ⁴Department of Orthopedic Surgery, Kochi Health Sciences Center, Kochi 781-8555, Japan; ⁵Department of Neurosurgery, Chikamori Hospital, Kochi 780-8522, Japan

Received July 25, 2024; Accepted October 17, 2024

DOI: 10.3892/ol.2024.14791

Abstract. Central nervous system (CNS) solitary fibrous tumors (SFTs) are rare but aggressive, often metastasizing to extracranial regions, with no established treatments apart from surgery. Pazopanib, a multikinase angiogenesis inhibitor, is used to treat extracranial SFTs; however, its efficacy for treating CNS SFTs remains unclear. To address this issue, the efficacy of pazopanib was investigated, focusing on tumor density and size in CNS SFTs with extracranial metastases after initiation, interruption or resumption of pazopanib treatment. The present study retrospectively reviewed 3 consecutive cases of CNS SFTs showing extracranial metastases that were referred to Kochi Health Sciences Center (Kochi, Japan) between January 2018 and April 2024 and were treated with pazopanib. All measurable lesions observed via contrast-enhanced computed tomography (CT; 50 lesions) and magnetic resonance imaging (MRI; 21 lesions) were evaluated. Cases 2 and 3, meeting the Choi criteria, showed

stable disease and achieved partial response after pazopanib initiation, respectively. In Case 1, both intracranial and extracranial tumor CT densities decreased after initiation and resumption of pazopanib treatment. However, both tumor CT sizes increased after interruption of pazopanib treatment. In Case 2, MRI revealed decreases and increases in the intracranial tumor size after initiation and interruption, respectively. Notably, pazopanib interruption caused rapid infratentorial tumor growth and death. Case 3 showed decreased extracranial tumor CT densities and sizes after pazopanib initiation, with pazopanib administered for 3.5 years. Thus, pazopanib may offer the potential to control both intracranial and extracranial tumors in patients with CNS SFTs with extracranial metastasis; however, treatment interruption requires careful consideration.

Introduction

According to the 2021 central nervous system (CNS) tumor classification by the World Health Organization (WHO), primary mesenchymal CNS tumors, including solitary fibrous tumors (SFTs), are rare and typically originate from the meninges (1). CNS SFTs show an age-adjusted incidence rate of 3.77 per 10,000,000 individuals (2), constituting 0.22% of all CNS tumors (3). A systematic review of 563 patients (average age, 41 years) revealed a slight predominance of CNS SFTs in males (55%, 246/450) and recurrence in 57% of cases (158/277) (4). Another systematic review found extracranial metastasis in 28% of cases (251/904), with a predilection for lung, liver, bone and pleural metastases (5). Additionally, WHO grade III was associated with a 1.88-fold increased risk of extracranial metastasis (5). The standard CNS SFT treatment involves surgery and adjunctive radiation therapy (6); however, CNS SFTs that metastasize to multiple extracranial lesions are not amenable to surgical resection, and radiation therapy for localized extra-meningeal SFTs does not extend the overall survival time (6). Furthermore, the efficacy of conventional chemotherapy is limited (6). No other standard treatment strategies have been established.

Correspondence to: Dr Takaya Tsuno, Department of Neurosurgery, Department of Radiology, Kochi Health Sciences Center, 2125-1 Ike, Kochi 781-8555, Japan
E-mail: tsunotak@gmail.com

Abbreviations: CNS, central nervous system; SFT, solitary fibrous tumor; CT, computed tomography; MRI, magnetic resonance imaging; WHO, World Health Organization; HPF, high-power field; EGR, early growth response; NAB, nerve growth factor I-A binding protein; STAT, signal transducer and activator of transcription; FGF, fibroblast growth factor; PDGF, platelet-derived growth factor; FGFR, FGF receptor; VEGF, vascular endothelial growth factor; VEGFR, VEGF receptor; KPS, Karnofsky Performance Status; PD, progressive disease; RECIST 1.1, Response Evaluation Criteria In Solid Tumors, version 1.1

Key words: CNS SFT, pazopanib, density, size, initiation, interruption, resumption

According to the 2021 WHO classification of CNS tumors, CNS SFTs are defined as ‘fibroblastic neoplasms’, categorized as ‘mesenchymal and non-meningothelial tumors’ (1). These tumors are graded as follows: Grade 1 [<5 mitoses/10 high-power fields (HPFs)], grade 2 (≥ 5 mitoses/10 HPF, without necrosis) and grade 3 (≥ 5 mitoses/10 HPF, with necrosis). Patients with CNS SFTs harbor the nerve growth factor I-A [also known as early growth response (EGR) 1] binding protein (NAB) 2::signal transducer and activator of transcription (STAT) 6 fusion gene, resulting from chromosomal inversion at the 12q13 locus (1). The classification suggests that CNS SFTs could be placed in the same group as pleural-origin SFTs; however, the precise cellular origin of CNS SFTs remains unclear (1).

NAB2 and STAT6 are localized to the nucleus and cytoplasm, respectively. However, immunostaining of CNS SFTs has revealed nuclear localization of STAT6 owing to the presence of the NAB2::STAT6 fusion gene, enabling their differentiation from meningiomas (1,7,8). The NAB2::STAT6 fusion protein, mediated by EGR1, activates target genes, including fibroblast growth factor (FGF) 2, platelet-derived growth factor (PDGF) D and receptor tyrosine kinases, including FGF receptor (FGFR) 1 and neurotrophic tyrosine receptor kinase 1, all involved in cell proliferation (9). The EGR1 target genes include vascular endothelial growth factor (VEGF) A and basic FGF, indicating their involvement in tumor angiogenesis (6).

Pazopanib, a tyrosine kinase inhibitor, has multiple targets, including VEGF receptor (VEGFR)1/2/3, PDGF receptor α/β and FGFR1/3 (10,11). In particular, pazopanib inhibits VEGFR2, further suppressing angiogenesis (11-13). Pazopanib demonstrated prolonged median progression-free survival in a phase 3 trial involving 369 patients with metastatic soft-tissue sarcoma (14); however, no patients with CNS SFT were included in the study. Therefore, while pazopanib exhibits significant efficacy against extracranial soft-tissue sarcoma, its effectiveness in CNS SFT remains unproven. Pazopanib has been approved for the treatment of advanced renal cell carcinoma and soft-tissue sarcoma in the United States and the European Union (11). Additionally, pazopanib may be considered in cases where extracranial SFTs originate from the pleura and are classified as malignant soft tissue tumors, despite the conventional restriction on pazopanib application for CNS SFTs; however, its efficacy in the treatment of CNS SFTs remains unclear. In the present study, 3 cases of high-grade CNS SFTs with multiple extracranial metastases that were treated with on-label pazopanib are described to examine the efficacy of pazopanib in treating CNS SFTs.

Case report

Cases. In total, 3 consecutive cases of CNS SFTs with multiple extracranial metastases were treated with pazopanib at Kochi Health Sciences Center between January 2018 and April 2024. The standard oral dose of pazopanib was set at 800 mg daily based on a previous phase 3 trial (14). A reduced dose of 600 mg daily was administered based on patient conditions or adverse events related to pazopanib, as reported previously in a phase 2 trial (15). Figs. S1 and S2 show the baseline whole-body images and representative pathological findings, respectively.

Case 1. A 51-year-old male patient who developed weakness in the right lower limb was diagnosed with a parasagittal sinus mass in December 2011. The patient underwent an initial tumor resection that same month and was diagnosed with atypical meningioma. Intracranial multifocal tumor regrowth necessitated multiple tumor resections and γ -knife treatments. The third tumor resection in September 2022 revealed a WHO grade 3 CNS SFT. After the sixth γ -knife therapy in October 2022, the patient was referred to Kochi Health Sciences Center with a Karnofsky Performance Status (KPS) of 60%. The patient exhibited right-hand dexterity impairment, right lower limb paresis and right lower limb sensory impairment. A whole-body computed tomography (CT) revealed multiple masses in the liver, pelvic cavity bones and a right cervical lymph node. A biopsy of the right sacral lesion confirmed SFT and pazopanib (800 mg daily) was initiated in January 2023. The pelvic cavity tumor was enlarged 2 months later, prompting a ~ 3 -week interruption of pazopanib treatment and the total resection of the enlarged tumor. Additional γ -knife therapy was administered for intracranial tumor growth in September 2023. Pazopanib was discontinued in October 2023 owing to an infection necessitating a sequestrectomy. In March 2024, both intracranial and extracranial residual tumors showed progressive disease (PD), necessitating additional γ -knife therapy. The enlarged sacral tumor reduced the KPS to 50% by April 2024, and heavy-ion radiotherapy was planned. The patient presented with worsening right lower limb paresis and pain from the right buttock to the right lower limb. A slowly enlarging liver lesion was also observed on a whole-body CT. Accordingly, heavy-ion radiotherapy (70.4 Gy, relative biological effectiveness, in 16 fractions) was administered for the right sacral lesion in June-July 2024, followed by stereotactic body radiotherapy (48 Gy in 4 fractions) for the liver lesion in August 2024. However, in September 2024, the patient presented with left facial paresis, dysphagia and left hemiparesis, and a whole-body CT revealed a rapid increase in multiple intracranial lesions. The patient refused all possible treatments, including the resumption of pazopanib, and palliative care was initiated. The patient experienced pazopanib-related adverse events of grade 3 diarrhea and grade 1 increase in serum bilirubin levels (1.3 mg/dl; normal range 0.2-1.2 mg/dl). The patient was treated with probiotics for diarrhea. Subsequently, the diarrhea and hyperbilirubinemia improved with the discontinuation of pazopanib.

Case 2. A 60-year-old female patient with dizziness and headache was initially diagnosed with a left infratentorial mass. The patient promptly underwent an initial tumor resection in September 2006 and was diagnosed with hemangiopericytoma. However, tumor regrowth, including a continuous extension to the left supratentorial region, necessitated a second resection with three γ -knife treatments by November 2022. Rapid tumor growth after the third γ -knife treatment led to the transfer of the patient to Kochi Health Sciences Center, with a KPS of 40%. The patient presented with impaired consciousness, aphasia and right hemiparesis. The patient promptly underwent a partial tumor resection of the rapidly enlarged left supratentorial tumor, confirmed as WHO grade 3 CNS SFT, in February 2023. A whole-body CT revealed multiple bone and lung metastases, and a biopsy of the thoracic vertebra 1 lesion confirmed SFT. Consequently, pazopanib (600 mg daily) was

Table I. Baseline tumor characteristics via computed tomography.

| Tumor characteristics | Case 1 | Case 2 | Case 3 | P-value |
|--|--------------------------------------|------------------------------------|--|--------------------|
| Tumor density (HU), [n (%)] | | | | |
| Intracranial | 85.75 (63.80-104.00), [16 (32.0)] | 77.45 (66.55-80.00), [4 (8.0)] | NA | 0.290 ^a |
| Extracranial | 97.85 (77.50-118.00), [4 (8.0)] | 82.90 (69.10-95.05), [7 (14.0)] | NA | 0.315 ^b |
| Extracranial | 97.85 (77.50-118.00), [4 (8.0)] | NA | 138.00 (126.00-143.00), [19 (38.0)] | 0.063 ^b |
| Extracranial | NA | 82.90 (69.10-95.05), [7 (14.0)] | 138.00 (126.00-143.00), [19 (38.0)] | 0.005 ^b |
| Tumor size (mm), [n (%)] | | | | |
| Intracranial | 7.38 (5.39-13.93), [16 (32.0)] | 24.36 (12.29-38.51), [4 (8.0)] | NA | 0.049 ^a |
| Extracranial | 11.52 (7.69-16.64), [4 (8.0)] | 20.79 (18.91-22.80), [7 (14.0)] | 16.24 (10.44-20.03), [19 (38.0)] | 0.226 ^c |
| Intracranial tumor locations, n (%) | | | | |
| Supratentorial | 16 (80) | 1 (5) | NA | 0.003 ^d |
| Infratentorial | 0 (0.0) | 3 (15) | NA | |

^aMann-Whitney U. ^bKruskal-Wallis with Holm multiple comparisons. ^cKruskal-Wallis. ^dFisher's exact test. Continuous variables are presented as medians and interquartile ranges. Italicized P-values denote statistical significance. HU, Hounsfield unit; NA, not available.

initiated on day 0. However, bleeding from the postoperative supratentorial lesion on day 6 resulted in a KPS of 30% and a 4-day interruption of pazopanib treatment. Eventually, the patient achieved stable disease on day 42 according to the Choi criteria (16). However, postoperative hydrocephalus necessitated further surgery, leading to a preoperative interruption of pazopanib on day 57. The patient showed improvement in right upper limb paresis. After removing the residual tumor in the left supratentorial region on day 65, the KPS score improved to 40%. However, rapid growth of the residual tumor in the left infratentorial region occurred on day 66, and the patient died on day 70. The pazopanib-related adverse event was a grade 3 intracranial hemorrhage.

Case 3. A 39-year-old female patient with diplopia was diagnosed with a large left frontal convexity tumor in September 2014 necessitating semi-emergency resection, revealing a WHO grade 2 hemangiopericytoma. Magnetic resonance imaging (MRI) conducted in September 2017 and 2018 revealed two skull lesions, prompting referral to Kochi Health Sciences Center, with a KPS of 100%. The patient did not exhibit any neurological deficits. An ¹⁸F-fluorodeoxyglucose positron emission tomography-CT scan performed in October 2018 revealed multiple liver, kidney and bone lesions. Consequently, the patient underwent posterior fixation for cervical vertebra 6 (C6) mass compression and a left sacral lesion biopsy, which confirmed a WHO grade 2 SFT/hemangiopericytoma. Denosumab (120 mg, subcutaneous injection every 4 weeks) was initiated that month for the treatment of multiple lytic bone lesions and proton therapy (65 Gy equivalent in 26 fractions) was administered to the enlarged soft tissue mass derived from C6. The patient presented with

numbness in the right fingers. Pazopanib (800 mg daily) was initiated in January 2019 but was reduced to 600 mg after 1 month owing to grade 2 hypertension. The patient had been on calcium channel blockers and angiotensin II inhibitors for blood pressure control prior to the initiation of pazopanib; however, due to an increase in blood pressure after pazopanib initiation, adjustments to these antihypertensive medications and a reduction in the pazopanib dosage were required to maintain blood pressure control. Partial response was achieved (according to the Choi criteria) in April 2019. The patient showed right-hand dexterity impairment in November 2019. Although pazopanib was administered for 3.5 years, PD necessitated treatment changes, including the administration of two chemotherapeutic agents: Trabectedin (1.2 mg/m²) in July 2022 and eribulin (1.4 mg/m²) in October 2023, followed by plans to resume pazopanib in April 2024, despite a KPS of 80%. The patient then exhibited right upper limb paresis. Throughout the 9 years, the patient did not experience a recurrence of the initial intracranial tumor. However, one of the two skull lesions protruded slightly outward and the extracranial soft tissue tumors progressed, whereas the lytic bone lesions transformed into sclerotic lesions, indicating disease stabilization. Pazopanib treatment was resumed in May 2024. A whole-body CT in June 2024 showed a decrease in the density of multiple systemic lesions; however, a whole-body CT in October 2024 indicated a subsequent increase in density. The tumor size exhibited a gradual tendency to increase.

Imaging assessments. In the present study, it was investigated how pazopanib affected the 3 cases. First, to assess the tumor backgrounds in the 3 cases, the baseline CT

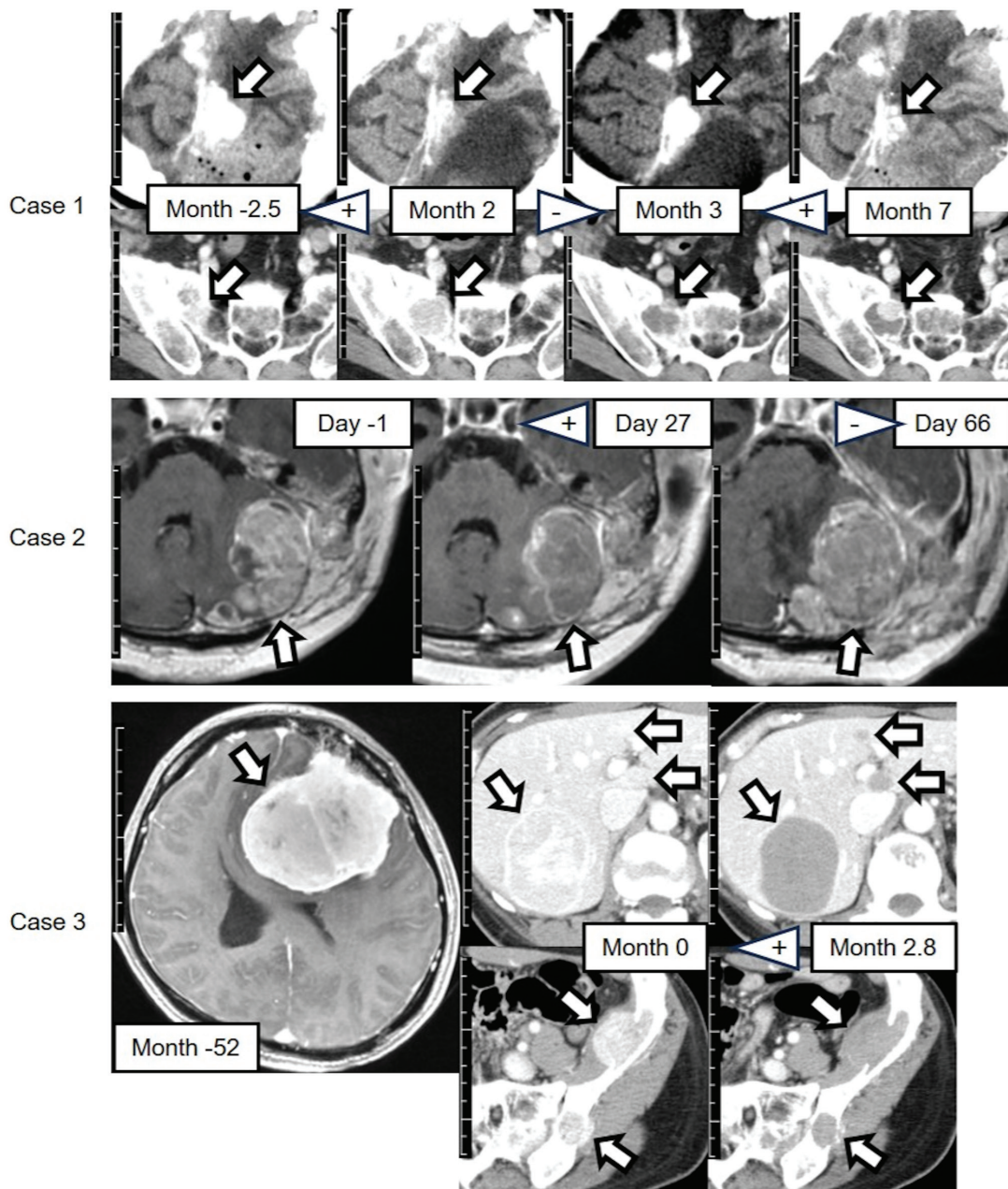


Figure 1. Contrast-enhanced CT or head T1-weighted images of the 3 cases. The arrows indicate the representative tumors. The months or days indicate the time since initiation of pazopanib treatment. + indicates initiation or resumption of pazopanib treatment; - indicates interruption of pazopanib treatment. Scale bar, 1 cm per division. Case 1: Upper row, left supratentorial falx tumors, head CT; lower row, right sacral tumor, pelvic CT. Case 2: T1-weighted images showing left infratentorial tumors. Case 3: Upper row, liver tumors, abdominal CT; lower row, left iliac tumors, pelvic CT; contrast-enhanced head T1-weighted image shows the initial primary tumor with no recurrence after resection. The image was provided by a previous institute, whose imaging equipment and conditions differed from those described in Appendix S1. CT, computed tomography.

tumor characteristics measured at Kochi Health Sciences Center were compared (Table I). The methods of the statistical analysis are detailed in Appendix S1. No significant difference was observed in the intracranial tumor densities between Cases 1 and 2 ($P=0.290$). However, the extracranial tumor density was higher in Case 3 than Case 2 ($P=0.005$), likely due to the inclusion of a lung lesion in Case 2 and the high-density range in Case 3. The intracranial tumor size was larger in Case 2 than Case 1 ($P=0.049$). Case 1 had only supratentorial tumors, whereas in Case 2, partial resection of the supratentorial tumor led to a predominance of infratentorial tumors ($P=0.003$). No significant differences

were observed in the extracranial tumor sizes among the three cases ($P=0.226$).

Subsequently, to evaluate the efficacy of pazopanib on intracranial and extracranial lesions in CNS SFT, imaging assessments pre- and post-treatment in the 3 cases were conducted. The details of the methods are provided in Appendix S1. Fig. 1 depicts the representative CT and MRI findings for each case. In all cases, by observational assessment, except for the right sacral tumor in Case 1, the CT density or MRI intensity decreased after pazopanib initiation or resumption and increased after interruption. Case 3 showed clear decreases in tumor CT densities after pazopanib

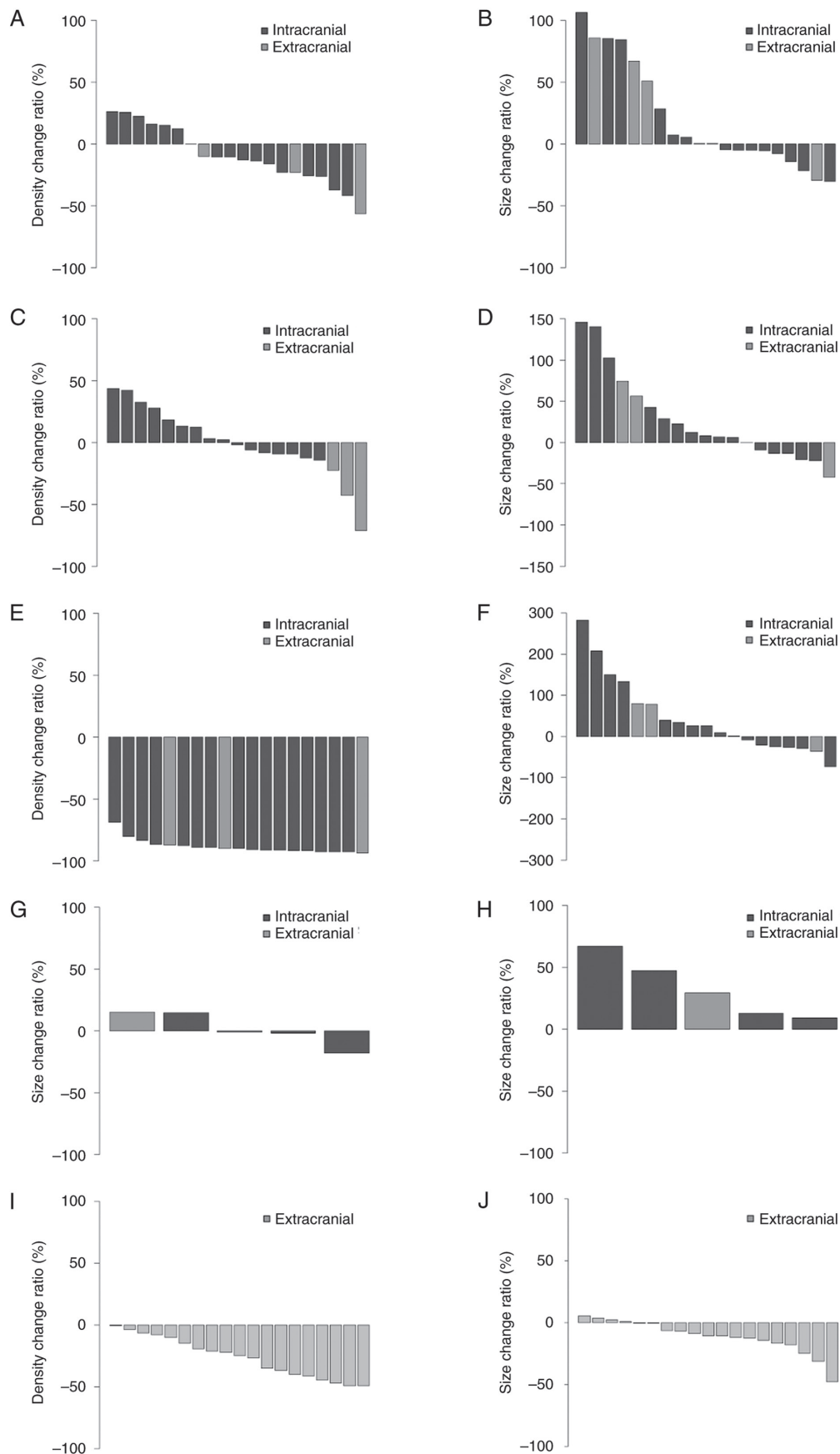


Figure 2. Waterfall plots display change ratios from pre- to post-pazopanib initiation, interruption or resumption. Distributions of (A) tumor density and (B) size change ratios in 20 CT lesions (intracranial, 16; extracranial, 4) in Case 1 after pazopanib initiation. Distributions of (C) tumor density and (D) size change ratios in 19 CT lesions (intracranial, 16; extracranial, 3) in Case 1 after pazopanib interruption. Distributions of (E) tumor density and (F) size change ratios in 19 CT lesions (intracranial, 16; extracranial, 3) in Case 1 after pazopanib resumption. Distributions of tumor size change ratios in 5 magnetic resonance imaging lesions (intracranial, 4; extracranial, 1) in Case 2 after pazopanib (G) initiation and (H) interruption. Distributions of (I) tumor density and (J) size change ratios in 19 extracranial CT lesions in Case 3 after pazopanib initiation. CT, computed tomography.

Table II. Literature review and comparison with cases in the present study.

| Authors, year | Age, years | Sex | WHO grade | Primary tumor sites in the CNS | Locations of metastases | Best overall response | | PFS, months | | Rapid tumor growth after pazopanib interruption | | OS, months | Prognosis (Refs.) |
|--|------------|-----|-----------|--------------------------------|---|-----------------------|-----------------|-------------|------|---|--------------|-----------------|-------------------|
| | | | | | | RECIST | Choi | RECIST | Choi | Intracranial | Extracranial | | |
| <i>Apra et al</i> , 2018 | 31 | M | 3 | Bil. Infratentorial | None | PR | NA | 4 | ND | ND | ND | ND | ND (17) |
| | 52 | F | 2 | Rt. temporal | ND | PR | NA | 6 | ND | ND | ND | ND | ND |
| <i>Maeda et al</i> , 2020 ^a | 52 | F | NA | Supra/infratentorial | Liver, lung | ND ^b | ND ^b | ND | ND | ND | ND | ND ^c | Dead (24) |
| Present study | 51 | M | 3 | Lt. parietal | Pelvic cavity, liver, bone, lymph node ^d | NA ^e | NA ^e | 2 | 2 | No | No | 16+ | Alive - |
| | 60 | F | 3 | Lt. infratentorial | Lung, bone | PD | SD | 1.4 | 1.4 | Yes | NA | 2.3 | Dead |
| | 39 | F | 2 | Lt. frontal | Liver, kidney, bone | SD | PR | 2.8 | 2.8 | No | No | 64+ | Alive |

^aOff-label use of temozolomide and bevacizumab before and after pazopanib treatment. ^bNot effective. ^c59 months after initiating temozolomide and bevacizumab. ^dIn the diagnosis of this lesion, reactive hyperplasia was considered as a differential diagnosis. ^eThe baseline contrast-enhanced computed tomography for Case 1 was obtained 2.5 months before pazopanib initiation, resulting in tumor enlargement during the pre-treatment period. The RECIST 1.1 and Choi criteria stipulate a baseline scan within 4 weeks prior to treatment initiation, resulting in NA. M, male; F, female; WHO, World Health Organization; NA, not available; CNS, central nervous system; Bil., bilateral; Rt., right; Lt., left; ND, not described; RECIST, Response Evaluation Criteria In Solid Tumors; PR, partial response; PD, progressive disease; SD, stable disease; PFS, progression-free survival; OS, overall survival.

initiation. In Case 1, by observational assessment, the size of the intracranial tumor decreased with pazopanib treatment and increased without it. In Case 2, the infratentorial tumors grew rapidly upon interruption of treatment, occupying the infratentorial region and compressing the brainstem.

To further evaluate the efficacy of pazopanib in the 3 cases, waterfall plots presenting the change ratios from pre- to post-pazopanib initiation, interruption or resumption were constructed (Fig. 2). The imaging evaluation methods are detailed in Appendix S1. In Case 1, after pazopanib initiation, most intracranial and extracranial tumor CT densities generally decreased (Fig. 2A). By contrast, the size of approximately half of the intracranial tumors and most of the extracranial tumors increased (Fig. 2B). Indeed, pazopanib was subsequently interrupted in Case 1 and surgical removal of an enlarged extracranial tumor was performed. Following interruption, the CT densities increased in approximately half of the intracranial tumors but decreased in all extracranial tumors (Fig. 2C). The size of most intracranial and extracranial tumors increased (Fig. 2D) but without rapid enlargement. In Case 1 after pazopanib resumption, the CT densities decreased in all intracranial and extracranial tumors (Fig. 2E). However, the size of more than half of the intracranial and extracranial tumors increased (Fig. 2F). In Case 2, contrast-enhanced head MRIs were used for the evaluation as contrast-enhanced whole-body CTs were not performed after pazopanib interruption. After pazopanib initiation in Case 2, the size of more than half of the intracranial tumors decreased, but an extracranial tumor (a left skull base bone lytic tumor) increased in size (Fig. 2G). However, after pazopanib interruption, all tumor sizes increased (Fig. 2H). The enlargement was rapid, leading to death. In Case 3, since there was no recurrence of the primary intracranial tumor, the evaluation focused solely on extracranial tumors based on a contrast-enhanced whole-body CT conducted 2.8 months after pazopanib initiation, as subsequent follow-up imaging was limited to plain whole-body CTs. After pazopanib initiation in Case 3, the CT densities decreased in all extracranial tumors (Fig. 2I), and the tumor size decreased in most extracranial tumors (Fig. 2J).

Discussion

CNS SFTs show high rates of extracranial metastasis (5), leading to unresectable systemically enlarging lesions that pose challenges in patient management. The results of the present study suggest a deviation from the typical surgical treatment approach, indicating a potential alternative strategy or response to the unique characteristics of CNS SFTs. The present study also clarified the changes in tumor density and/or size from pre- to post-pazopanib initiation, emphasizing the significant concerns regarding pazopanib interruption. This is clinically important and noteworthy, as it has not been previously reported in studies on patients with CNS SFTs.

Pazopanib efficacy has been assessed in a phase 3 trial of 369 patients with metastatic soft-tissue sarcoma without CNS involvement (14). The median progression-free survival was 4.6 months in patients who underwent pazopanib therapy, significantly surpassing that observed with the placebo (1.5 months), whereas the median overall survival did not increase after pazopanib therapy. Pazopanib was also tested

in a phase 2 trial for systemic SFTs in 36 patients, 5 of whom had meningeal involvement (15). However, the efficacy of pazopanib in CNS SFTs has not been individually assessed. Pazopanib is preferred for the treatment of SFTs but not for CNS SFTs, according to the National Comprehensive Cancer Network Guidelines version 1.2024 (<https://www.nccn.org/>). Pazopanib was shown to reduce the intracranial SFT volumes in 2 cases (WHO grades 2 and 3) after 4-6 months (17). Another study reported that extracranial metastatic lesions shrank after 3-4 months of pazopanib therapy (18). Grade 3-4 adverse events of pazopanib treatment include hypertension (3-29%), lymphopenia (4-14%), diarrhea (4-8%), elevated alanine aminotransferase (0-19%), aspartate aminotransferase (2-8%) and bilirubin (0-6%) levels, bleeding (2%), hypoglycemia (0-5%), hyperglycemia (0-3%) (12), pneumothorax (2-3%), and thrombocytopenia (2-3%) (19). In the present study, the adverse events associated with pazopanib were assessed according to the Common Terminology Criteria for Adverse Events, version 5.0 (20). However, the criteria do not specify clear discontinuation guidelines for the medication, and we considered the following: Case 1 had grade 3 diarrhea and grade 1 hyperbilirubinemia, which resolved after pazopanib discontinuation. Antidiarrheal agents were also required for the management of diarrhea. Case 2 had postoperative grade 3 intracranial hemorrhage, necessitating temporary interruption, whereas Case 3 required a pazopanib dose reduction and increased antihypertensive treatment due grade 2 hypertension. Thus, managing the adverse events required interruption, discontinuation, dose reduction and symptomatic treatments. Interruption and discontinuation may require prompt resumption and medication changes, as demonstrated in Cases 2 and 3, respectively; however, the changes have limitations regarding medication selection. The mechanisms by which pazopanib causes diarrhea, hemorrhage and hypertension have been proposed as submucosal fat accumulation in the gastrointestinal tract (21), targeting kinase events downstream of glycoprotein VI and other platelet receptors (22), imbalance in vasoconstrictors and vasodilators, capillary depletion and direct renal impairment (23).

A PubMed (<https://pubmed.ncbi.nlm.nih.gov/>) search for English-language literature published between January 2000 and April 2024 was conducted using the terms 'meninges', 'solitary fibrous tumor', 'hemangiopericytoma' and 'pazopanib'. The search yielded only two previous studies (17,24); a comparison with the cases of the present study is summarized in Table II. Maeda *et al* (24) reported the off-label use of temozolomide and bevacizumab in 4 SFT cases, including only 1 CNS SFT case additionally treated with pazopanib. The treatment response was evaluated based on the Response Evaluation Criteria in Solid Tumors, version 1.1 (RECIST 1.1) (6,25) and Choi criteria. However, several results from these studies were unavailable. Shorter progression-free survival was observed in the present study compared with that observed in the Apra *et al* study (17), although the efficacy of pazopanib was comparable between the two studies.

A case report of uterine carcinosarcoma with right lung metastasis described rapid tumor growth following pazopanib interruption; tumor reduction was observed following pazopanib resumption, suggesting the benefit of early pazopanib resumption after interruption (26). In the present study, Case

1 experienced some pazopanib interruptions but no rapid growth, whereas Case 2 exhibited rapid growth upon pazopanib interruption. By contrast, trabectedin was promptly initiated in Case 3 upon discontinuation of pazopanib, resulting in no rapid growth. Thus, pazopanib interruption does not necessarily induce rapid growth. The critical factors for rapid growth following interruption remain unclear. However, dose reduction or prompt medication changes may help prevent rapid growth. Regarding tumor growth and mortality after interruption, the supratentorial lesions in Case 1 were enlarged without mortality. By contrast, the infratentorial lesions in Case 2 were enlarged with perifocal edema, causing fatal brainstem compression. Case 2 had larger baseline tumors than those of Case 1, and growth in a confined infratentorial region could have contributed to the mortality.

Nevertheless, the present study has some limitations. First, the baseline contrast-enhanced CT for Case 1 was obtained 2.5 months before pazopanib initiation (Table SI) and the tumor sizes increased during this time. This explains the large tumor size changes from pre- to post-pazopanib initiation. This also diverged from strict adherence to the RECIST 1.1 and Choi criteria. Follow-up imaging periods varied across the cases (Table SI). Case 3 underwent only one follow-up contrast-enhanced whole-body CT. Therefore, consistent follow-up imaging is required in further studies. Second, normalization was not feasible for evaluating quantitative MRI intensity changes owing to variations in the machines and imaging conditions for MRI. Thus, further evaluation with MRI may be required. Third, in Case 3, denosumab caused sclerotic lytic bone lesions, possibly affecting the efficacy of pazopanib. However, denosumab is ineffective for soft tissue lesions. Fourth, the present study describes the experience of only 3 cases, and it does not assess the robustness or generalizability of the results. Fifth, prognostic tumor biomarkers for CNS SFTs have not been established. Interferon-stimulated gene 15 (27) and p53 (28) have been reported as potential prognostic factors for SFTs; however, there has been no specific mention for CNS SFTs. The present study lacked data on these biomarkers, necessitating further investigation.

In conclusion, pazopanib may inhibit both intracranial and extracranial tumor growth in CNS SFTs with multiple extracranial metastases. In the present study, 1 patient received pazopanib for >3 years. Further research and case studies are required to determine the efficacy of pazopanib. However, caution is warranted regarding rapid tumor growth following pazopanib interruption. Thus, abrupt interruption should be avoided and gradual tapering or prompt transition to alternative agents is recommended.

Acknowledgements

The authors would like to thank Dr Jun Iwata and Dr Manabu Matsumoto (Department of Pathology, Kochi Health Sciences Center, Kochi, Japan) for providing the pathological images, Mr. Yuichi Taniguchi (Department of Medical Technology, Kochi Health Sciences Center, Kochi, Japan) for supplying the pathology protocols, and Mr. Masaki Oka and Mr. Yoshiaki Wada (Department of Medical Technology, Kochi Health Sciences Center, Kochi, Japan) for their assistance in preparing the CT and MRI protocols.

Funding

No funding was received.

Availability of data and materials

The data generated in the present study may be requested from the corresponding author.

Authors' contributions

TT, NM, KN and HI conceptualized and designed the study, developed the data collection instruments, collected data, conducted the initial analyses, analyzed, interpreted and validated the data as well as reviewed and revised the manuscript. NK, DY, YK, TM and HN coordinated and supervised the data collection and validation and reviewed the manuscript. TT drafted the manuscript. All authors have read and approved the final version of the manuscript. TT and HI confirm the authenticity of all the raw data.

Ethics approval and consent to participate

This study was performed in-line with the principles of the Declaration of Helsinki. Approval was granted by the Ethics Committee of Kochi Health Sciences Center (Kochi, Japan; date: February 13, 2024; approval no. 231080). We declare that this study complies with the CARE reporting guidelines. Written informed consent was obtained from the patients or from family members if the patient had passed away.

Patient consent for publication

Research participants provided informed consent for the publication of the manuscript and images.

Competing interests

The authors declare that they have no competing interests.

Authors' information

Takaya Tsuno ORCID ID: 0000-0002-9446-2374

References

1. WHO Classification of Tumours Editorial Board: Mesenchymal, non-meningothelial tumours involving the CNS. In: Central Nervous System Tumours, WHO Classification of Tumours (5th edition). International Agency for Research on Cancer, Lyon, pp299-305, 2021.
2. Kinslow CJ, Bruce SS, Rae AI, Sheth SA, McKhann GM, Sisti MB, Bruce JN, Sonabend AM and Wang TJC: Solitary-fibrous tumor/hemangiopericytoma of the central nervous system: A population-based study. *J Neurooncol* 138: 173-182, 2018.
3. Trifiletti DM, Mehta GU, Grover S and Sheehan JP: Clinical management and survival of patients with central nervous system hemangiopericytoma in the national cancer database. *J Clin Neurosci* 44: 169-174, 2017.
4. Rutkowski MJ, Sughrue ME, Kane AJ, Aranda D, Mills SA, Barani IJ and Parsa AT: Predictors of mortality following treatment of intracranial hemangiopericytoma. *J Neurosurg* 113: 333-339, 2010.

5. Ratneswaren T, Hogg FRA, Gallagher MJ and Ashkan K: Surveillance for metastatic hemangiopericytoma-solitary fibrous tumors-systematic literature review on incidence, predictors and diagnosis of extra-cranial disease. *J Neurooncol* 138: 447-467, 2018.
6. de Bernardi A, Dufresne A, Mishellany F, Blay JY, Ray-Coquard I and Brahmi M: Novel therapeutic options for solitary fibrous tumor: Antiangiogenic therapy and beyond. *Cancers (Basel)* 14: 1064, 2022.
7. Schweizer L, Koelsche C, Sahn F, Piro RM, Capper D, Reuss DE, Pusch S, Habel A, Meyer J, Göck T, *et al*: Meningeal hemangiopericytoma and solitary fibrous tumors carry the NAB2-STAT6 fusion and can be diagnosed by nuclear expression of STAT6 protein. *Acta Neuropathol* 125: 651-658, 2013.
8. Gao F, Ling C, Shi L, Commins D, Zada G, Mack WJ and Wang K: Inversion-mediated gene fusions involving NAB2-STAT6 in an unusual malignant meningioma. *Br J Cancer* 109: 1051-1055, 2013.
9. Robinson DR, Wu YM, Kalyana-Sundaram S, Cao X, Lonigro RJ, Sung YS, Chen CL, Zhang L, Wang R, Su F, *et al*: Identification of recurrent NAB2-STAT6 gene fusions in solitary fibrous tumor by integrative sequencing. *Nat Genet* 45: 180-185, 2013.
10. Pottier C, Fresnais M, Gilon M, Jérusalem G, Longuespée R and Sounni NE: Tyrosine Kinase inhibitors in cancer: Breakthrough and challenges of targeted therapy. *Cancers (Basel)* 12: 731, 2020.
11. Zhao Y and Adjei AA: Targeting angiogenesis in cancer therapy: Moving beyond vascular endothelial growth factor. *Oncologist* 20: 660-673, 2015.
12. Hamberg P, Verweij J and Sleijfer S: (Pre-)clinical pharmacology and activity of pazopanib, a novel multikinase angiogenesis inhibitor. *Oncologist* 15: 539-547, 2010.
13. Kumar R, Knick VB, Rudolph SK, Johnson JH, Crosby RM, Crouthamel MC, Hopper TM, Miller CG, Harrington LE, Onori JA, *et al*: Pharmacokinetic-pharmacodynamic correlation from mouse to human with pazopanib, a multikinase angiogenesis inhibitor with potent antitumor and antiangiogenic activity. *Mol Cancer Ther* 6: 2012-2021, 2007.
14. van der Graaf WT, Blay JY, Chawla SP, Kim DW, Bui-Nguyen B, Casali PG, Schöffski P, Aglietta M, Staddon AP, Beppu Y, *et al*: Pazopanib for metastatic soft-tissue sarcoma (PALETTE): A randomised, double-blind, placebo-controlled phase 3 trial. *Lancet* 379: 1879-1886, 2012.
15. Martin-Broto J, Stacchiotti S, Lopez-Pousa A, Redondo A, Bernabeu D, de Alava E, Casali PG, Italiano A, Gutierrez A, Moura DS, *et al*: Pazopanib for treatment of advanced malignant and dedifferentiated solitary fibrous tumour: A multicentre, single-arm, phase 2 trial. *Lancet Oncol* 20: 134-144, 2019.
16. Choi H, Charnsangavej C, Faria SC, Macapinlac HA, Burgess MA, Patel SR, Chen LL, Podoloff DA and Benjamin RS: Correlation of computed tomography and positron emission tomography in patients with metastatic gastrointestinal stromal tumor treated at a single institution with imatinib mesylate: Proposal of new computed tomography response criteria. *J Clin Oncol* 25: 1753-1759, 2007.
17. Apra C, Alentorn A, Mokhtari K, Kalamarides M and Sanson M: Pazopanib efficacy in recurrent central nervous system hemangiopericytomas. *J Neurooncol* 139: 369-372, 2018.
18. Lee SJ, Kim ST, Park SH, Choi YL, Park JB, Kim SJ and Lee J: Successful use of pazopanib for treatment of refractory metastatic hemangiopericytoma. *Clin Sarcoma Res* 4: 13, 2014.
19. Nakamura T, Matsumine A, Kawai A, Araki N, Goto T, Yonemoto T, Sugiura H, Nishida Y, Hiraga H, Honoki K, *et al*: The clinical outcome of pazopanib treatment in Japanese patients with relapsed soft tissue sarcoma: A Japanese musculoskeletal oncology group (JMOG) study. *Cancer* 122: 1408-1416, 2016.
20. Common Terminology Criteria for Adverse Events (CTCAE). V5.0, 2017. https://ctep.cancer.gov/protocoldevelopment/electronic_applications/docs/ctcae_v5_quick_reference_5x7.pdf.
21. Liu J, Yan S, Du J, Teng L, Yang R, Xu P and Tao W: Mechanism and treatment of diarrhea associated with tyrosine kinase inhibitors. *Heliyon* 10: e27531, 2024.
22. Tullemans BME, Nagy M, Sabrkhany S, Griffioen AW, Oude Egbrink MGA, Aarts M, Heemskerk JWM and Kuijpers MJE: Tyrosine kinase inhibitor pazopanib inhibits platelet procoagulant activity in renal cell carcinoma patients. *Front Cardiovasc Med* 5: 142, 2018.
23. Justice CN, Derbala MH, Baich TM, Kempton AN, Guo AS, Ho TH and Smith SA: The impact of pazopanib on the cardiovascular system. *J Cardiovasc Pharmacol Ther* 23: 387-398, 2018.
24. Maeda O, Ohka F, Maesawa S, Matsuoaka A, Shimokata T, Mitsuma A, Urakawa H, Nakamura S, Shimoyama Y, Nakaguro M, *et al*: Solitary fibrous tumor/hemangiopericytoma treated with temozolomide plus bevacizumab: A report of four cases and literature review. *Nagoya J Med Sci* 82: 631-644, 2020.
25. Eisenhauer EA, Therasse P, Bogaerts J, Schwartz LH, Sargent D, Ford R, Dancey J, Arbuck S, Gwyther S, Mooney M, *et al*: New response evaluation criteria in solid tumours: Revised RECIST guideline (version 1.1). *Eur J Cancer* 45: 228-247, 2009.
26. Sawayama S, Murakami R, Aki M, Kawaguchi Y, Takao Y, Nonogaki H, Goto T and Yamauchi C: Efficacy of pazopanib in FGFR1-amplified uterine carcinosarcoma: A case report. *Gynecol Oncol Rep* 41: 100993, 2022.
27. Mondaza-Hernandez JL, Moura DS, Lopez-Alvarez M, Sanchez-Bustos P, Blanco-Alcaina E, Castilla-Ramirez C, Collini P, Merino-Garcia J, Zamora J, Carrillo-Garcia J, *et al*: ISG15 as a prognostic biomarker in solitary fibrous tumour. *Cell Mol Life Sci* 79: 434, 2022.
28. Napolitano A, Moura DS, Hindi N, Mondaza-Hernandez JL, Merino-Garcia JA, Ramos R, Dagrada GP, Stacchiotti S, Graziano F, Vincenzi B and Martin-Broto J: Expression of p53 as a biomarker of pazopanib efficacy in solitary fibrous tumours: Translational analysis of a phase II trial. *Ther Adv Med Oncol* 14: 17588359221116155, 2022.
29. Kanda Y: Investigation of the freely available easy-to-use software 'EZ' for medical statistics. *Bone Marrow Transplant* 48: 452-458, 2013.
30. Giannini C, Rushing EJ, Hainfellner JA, Bouvier C, Figarella-Branger D, von Deimling A, Wesseling P and Antonescu CR: Solitary fibrous tumour/haemangiopericytoma. In: WHO Classification of Tumours of the Central Nervous System (Revised 4th edition). International Agency for Research on Cancer, Lyon, pp248-254, 2016.



Copyright © 2024 Tsuno et al. This work is licensed under a Creative Commons Attribution-NonCommercial-NoDerivatives 4.0 International (CC BY-NC-ND 4.0) License.